Proceedings of the 21st ICSMGE, Vienna, Austria, 14 – 19 June 2026. Pistrol, Adam & Schweiger (eds.)
Published by: ÖGG, Austrian Society for Geomechanics, Salzburg, Austria, ISBN 978-3-9503898-4-5
https://doi.org/10.53243/ICSMGE2026-1093

Augmenting the role of soil test database in efficient reliability-based design of ultimate and serviceability limit states

Man Kong Lo
Department of Civil and Environmental Engineering, The Hong Kong Polytechnic University, Hong Kong SAR, man-kong.lo@polyu.edu.hk

Andy Yat Fai Leung
Department of Civil and Environmental Engineering, The Hong Kong Polytechnic University, Hong Kong SAR, andy.yf.leung@polyu.edu.hk

ABSTRACT: In Hong Kong, extensive datasets of triaxial test results of local soil specimens are available in an online repository system maintained by the government. Although the data were from various projects, the laboratory testing procedures are consistent as they follow the standard local practice. A database of over 3,000 data for various soils was compiled, resulting in the probability density functions of Mohr-Coulomb effective shear strength parameters (effective cohesion, c' and effective friction angle, ϕ'). This regional distribution is useful as prior knowledge for reliability-based design. For example, reliability-based design for soil-nailed slopes can be efficiently performed using design charts derived from the regional distribution of c' and ϕ'. When limited site-specific data are available at a site, they can be assimilated with regional distribution through the hierarchical Bayesian modelling method, with the aim of reducing the statistical uncertainty of the probability distribution. In general, this would lead to a more cost-effective reliability-based design, unless the site shear strength is distinctively weaker than the regional average. Apart from the assessment of ultimate limit state, triaxial test database can be utilized to assess serviceability limit state. To this end, stress path information of 98 sets of multi-stage consolidated-undrained triaxial compression tests (multi-stage CU) are digitized from scanned reports, using optical character recognition from Excel and ChatGPT-4o. CUM test provides three separate stress paths for the same soil specimen. When this characteristic is combined with the critical state soil model Norsand, the small-strain shear modulus (Gmax) and critical state parameters (Γ, λ, Mtc) can be reasonably calibrated, which are essential parameters for predicting soil deformation. This project shows that, by utilizing geotechnical data in various scales, a data-centric platform can be constructed, which can promote data-driven geotechnical design for both ultimate and serviceability limit states.

KEYWORDS: Triaxial test, database, Bayesian updating, reliability-based design, critical-state soil model.

1 INTRODUCTION

Reliability-based geotechnical design aims to achieve a target reliability index or failure probability, taking into consideration the uncertainties associated with soil and rock properties, the loading and groundwater conditions, and the numerical models. Recently there is an increased focus to include full reliability methods (in contrast to the semi-reliability methods such as partial factors) in international standards such as Eurocode 7 or ISO 2394, with technical committees such as TC304 dedicated to promote reliability-based design. The authors identified the following challenges associated with the further widespread use of reliability design methods:

1. Provide accurate probability distribution functions (PDF) for the geotechnical uncertainties for practitioners;
2. Utilize site-specific data to refine or improve the reliability-based design;
3. Develop efficient reliability design methods with relatively low computational cost;
4. Calibrating the target reliability index for the ultimate limit state (ULS) and/or serviceability limit state (SLS) of concern;

This paper will mainly discuss items 1 to 3, summarizing and elaborating the recent researches by the authors and the Hong Kong Geotechnical Engineering Office (GEO), and using the soil testing data in Hong Kong as the reference. First, a regional PDF of soil shear strength parameters will be established from a database of over 3000 test data. The PDF for soil stiffness parameters (Young's modulus and small-strain shear modulus) and critical state parameters are also included. Next, the paper discusses the use of Bayesian methods to construct a prior PDF of soil properties, with can be incorporated with site data through Bayesian updating to produce a refined PDF of soil properties. Finally, illustrative examples of reliability-based design for both ULS and SLS are presented, together with an efficient design chart method for ULS design.

2 REGIONAL PDF OF SOIL PARAMETERS

2.1 *Soil shear strength parameters*

The PDF of soil parameters can be established through a territory-wide database of relevant testing data (Chan et al. 2022). In Hong Kong, extensive triaxial test results of soil specimens are available in an online repository system maintained by the government, known as Geotechnical Information Infrastructure (GInfo). Over 3000 data of various soil types are retrieved from more than 200 slope projects across Hong Kong. These soils include superficial deposits: colluvium (COLL), fill (FILL); and in-situ soils: completely decomposed granite (CDG), completely decomposed volcanics (CDV) and residual soil from granitic origin (RS granitic) and volcanic origin (RS volcanic). Specifically, the triaxial test considered is multi-staged CU (consolidated undrained) test, where a soil sample is subjected to three stages of isotropic consolidation and undrained shearing. In each stage, the specimen was consolidated at a fixed effective confining pressure and loaded until the failure criterion, which is defined as the maximum effective principal stress ratios (σ1/σ3), was reached. After that, the specimen would be re-consolidated at a higher effective confining pressure and then subjected to loading again. At the third (final) shearing stage, the test would be terminated at the axial strain of 20% instead. Therefore, Mohr-Coulomb shear strength parameters (effective cohesion, c' and effective friction angle, ϕ') can be determined by linear regression of the three peak stress states in the same test. Although the soil data were from various projects, the multi-staged CU procedures are consistent as they follow the standard local practice stipulated in Geospec 3. Table 1 summarizes the

statistics (mean μ, standard deviation σ, correlation coefficient ρ), and the formulated PDFs of the c'-ϕ' parameters. c' can be reasonably fitted by gamma distribution with shape parameter α and rate parameter β; while ϕ' can be reasonably fitted by a normal distribution. In addition, correlation between c' and tan ϕ' ranges from moderately negative (-0.423) to weakly positive (0.123).

Table 1. Regional statistics of the soil shear strength database

Soil Type	Data size	Cohesion (c')			Friction Angle (ϕ')		ρ between c' and $\tan\phi'$
		μ_c (kPa)	σ_c (kPa)	α, β	μ_ϕ (°)	σ_ϕ (°)	
CDG	750	11.9	7.6	2.0 6.8	37.6	5.2	0.123
CDV	650	11.4	7.4	2.5 4.8	35.1	4.5	-0.120
RS Granitic	300	7.6	5.1	2.1 4.1	32.4	4.6	-0.451
RS Volcanic	150	9.4	6.6	1.6 6.6	32.8	4.9	-0.302
Fill	650	6.6	5.5	1.3 5.0	34.1	5.0	-0.159
COLL	800	7.9	6.1	1.8 4.6	34.2	4.7	-0.189

2.2 *Soil stiffness parameters*

The above shear strength parameters only utilize the data of the peak stress states. It is possible to extract more useful attributes, in particular the soil stiffness parameters, by using the entire stress path of the multi-stage CU test. To this end, stress path and shear stress-strain curves of 98 sets of multi-stage CU test of Hong Kong CDG are digitized from scanned reports in pdf format. This project first uses the optical character recognition tool in MS Excel. Later, it was found that using ChatGPT-4o brings a higher digitization accuracy. Specifically, the input into ChatGPT-4o includes the image of the tabular data on the entire stress path and stress-strain curve, and a prompt to instruct ChatGPT-4o to display the extracted data in compatible with MS Excel. After digitization, the Mohr-Coulomb model parameters (i.e. Young's modulus E and dilation angle δ, since c' and ϕ' are already fitted) are then calibrated by minimizing the difference between the simulated and experimental stress-strain curves, through a custom-made cost function. An Excel spreadsheet tool has been developed for efficient calibration. Figure 1 shows the calibration results for a set of multi-stage CU test data.

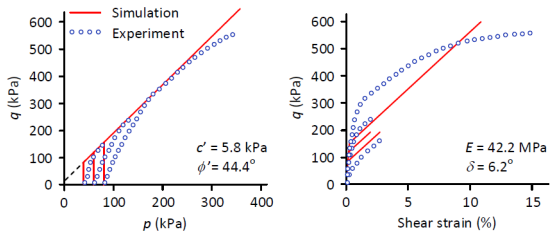

Figure 1. Multi-stage CU test result of CDG specimen with calibration by Mohr-Coulomb model.

After calibration of model parameters, Figure 2 (left) shows the histogram of the E values, with mean of 40.2MPa and SD of 18.2MPa. E can be reasonably fitted by a truncated normal distribution. The range of E concurs with the suggested ranges in Geoguide 1 (GEO 2020) (5-20MPa for loose sand; 16-40MPa for medium dense sand; 30-100MPa for dense sand). Apart from Mohr-Coulomb model, the stress paths can also be fitted with a more sophisticated constitutive model which accounts for the non-linearity of soil stiffness. Under this method, the elastic parameter (A) is indirectly calibrated through matching the elasto-plastic stress-strain response during undrained triaxial shearing. Figure 2 (right) shows the calibrated lognormal distribution for the parameter A, with mean 12.8MPa and SD 6MPa. Parameter A is related to the small-strain shear modulus Gmax by:

$$G_{max} = A\frac{(2.17-e)^2}{1+e}\left(\frac{p}{100}\right)^{0.5} \quad (1)$$

where e is the void ratio and p is the mean effective stress.

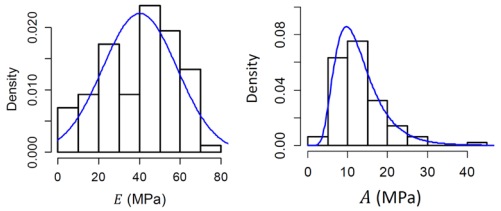

Figure 2. Distribution of stiffness parameters for Hong Kong CDG

2.3 *Soil critical state parameters*

Understanding the critical state of soil is important to predict the soil dilatancy, the soil deformation subjected to a large loading, and the soil stability under cyclic loading. Critical state can be described via a critical state line (CSL) in the e-lnp space, and a critical stress ratio in triaxial compression condition (Mtc). CSL follows a semi-log form with intercept Γ and slope λ, while Mtc is related to the critical friction angle by $\sin\phi_{cv} = 3M_{tc}/(6+M_{tc})$.

To calibrate the critical state parameters from multi-stage CU test data, the NorSand constitutive model (Jefferies 1993) is used. NorSand model had been shown to be capable of capturing the behaviour of silty and sandy materials under various confining stress and soil densities. The key component in NorSand model is the state parameter, which is a distance measure from the current soil state to the critical state. Adopting the NorSand model, critical state parameters can be calibrated by minimizing the custom-made cost function. Figure 3 shows the resulting distributions for Γ, λ and M_{tc} from the 98 sets of multi-stage CU test data, while Table 2 summarizes their statistics and their PDF form.

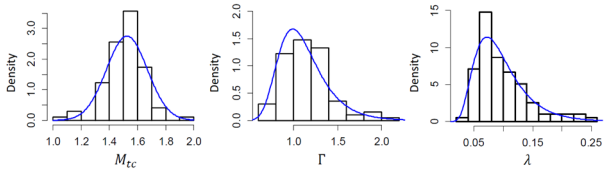

Figure 3. Distribution of critical state parameters for Hong Kong CDG

Table 2. Regional PDF for critical state parameters of Hong Kong CDG

Parameter	Mean	SD	PDF
Γ	1.146	0.269	Lognormal
λ	0.1	0.045	Lognormal
M_{tc}	1.533	0.139	Normal

3 ASSIMILATE SITE DATA WITH THE RERIONAL PDF THROGUH BAYESIAN UPDATING

The "regional PDF" in previous section can be thought as a pooled distribution of soil parameters from many sites of similar geologic conditions across a region. However, the distribution at a particular site, known as "site-specific PDF", may deviate from the regional PDF in a certain extent. For example, Figure 4 shows the scatterplot of c'- ϕ' of Hong Kong

CDG with different symbols for different sites, and the corresponding 95% credible region for each site (i.e. 95% of the data points are expected to be within the credible region). Compared to the credible region of the regional PDF (blue dashed line), it is evident that the site-specific PDF can deviate from the regional PDF.

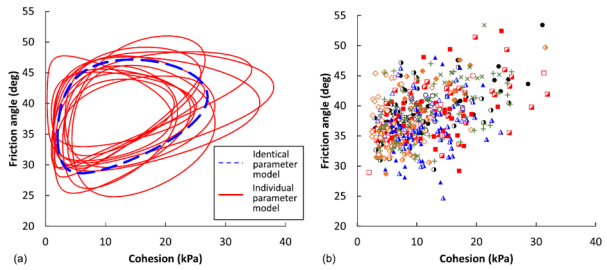

Figure 4. (left) 95% credible regions and (right) scatterplot of c'- ϕ' of Hong Kong CDG among different sites

Although the site-specific PDF can be formulated with a relatively small uncertainty with more than 20 site data points, often this cannot be achieved in daily practice. Under limited amount of site data, Bayesian updating is a proper framework for assimilating site data with the existing information, and the core formula is:

$$f(\theta|y) = kL(\theta)f(\theta) \tag{2}$$

where θ are the parameters of interest (such as μ or σ); $f(\theta)$ is the prior PDF of θ; $L(\theta)$ is the likelihood of observing the site data y; k is the normalizing constant; and $f(\theta|y)$ is the Bayesian updated (or posterior) PDF of θ. Conceptually, with very limited site-specific data, the posterior PDF would resemble the regional PDF, and it would approach the site-specific PDF with increasing amount of site information.

To establish the prior PDF, the authors adopted another Bayesian technique, namely the Hierarchical Bayesian model (HBM) (Lo et al. 2024), which can decompose the total variability of soil properties into the "variability within a site" and "variability between the sites". Figure 5 displays the multi-leveled structure of the HBM model, where each site has a different set of statistical parameters (such as $\mu_{c,i}, \sigma_{c,i}$), and there are hyperparameters (such as m_{μ_c}, p_{μ_c}) to govern the variations of statistical parameters among the sites.

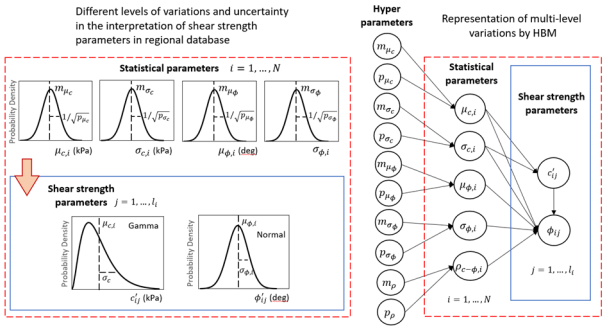

Figure 5. Hierarchical Bayesian model for the regional shear strength data.

As mentioned, soil data is taken from registered slopes in Hong Kong, and each slope has a location index indicating one of the 64 zones across the city. By treating each zone as a "site" in the HBM context, HBM model is fitted through a Gibbs sampling procedure, and the prior PDF be established based on the hyperparameters of the HBM model. Table 3 shows the prior PDF for the Hong Kong CDG parameters, which can be readily applied in Equation (1) for Bayesian updating. The data-likelihood is simply the probability density of the site data (gamma density for c' and normal density for ϕ').

Table 3. Prior PDF for the statistical parameters of c'-ϕ' of Hong Kong CDG

Parameter	Prior PDF
μ_c (kPa)	N(11.9, 1.94)
σ_c (kPa)	N(6.26,0.29)
μ_ϕ (°)	N(37.6,1.41)
σ_ϕ (°)	N(4.41,0.86)
$\rho_{c-\phi}$	N(0.327,0.167)

Given the prior PDF and data likelihood, the posterior PDF $f(\theta|y)$, and subsequently the predictive PDF $f(y_{new}|y)$ for soil properties at the site, can be evaluated by numerical methods implemented in various software, such as the BEST Excel VBA tool (Wang et al. 2016), or the Just Another Gibbs Sampler (JAGS) package in the R software (Lo et al. 2024). Alternatively, simplified expressions for the mean and SD of y_{new} can be derived, by utilizing the theory of the conjugate priors (Lo and Leung 2025). For the case of Hong Kong CDG:

$$\mu_{c,new} = 48\frac{\exp(\mu_n - 1.1)}{1+\exp(\mu_n - 1.1)}$$

$$\sigma_{c,new} \approx 7.6$$

$$\mu_{\phi,new} = 37.6 + 5.2\mu_n$$

$$\sigma_{\phi,new} = 5.2\sqrt{\frac{\beta_n(\lambda_n+1)}{\lambda_n(\alpha_n-1)}} \tag{3}$$

where

$$\mu_n = \frac{\lambda_0\mu_0 + n\bar{y}}{\lambda_0 + n}$$

$$\lambda_n = \lambda_0 + n$$

$$\alpha_n = \alpha_0 + \frac{n}{2}$$

$$\beta_n = \beta_0 + \frac{1}{2}\left[(n-1)s_y + \frac{n\lambda_0}{\lambda_0+n}(\bar{y}-\mu_0)^2\right] \tag{4}$$

where $\bar{y}$ and s_y are the sample mean and variance of the site data respectively, and n is the size of site data. $(\mu_0, \lambda_0, \alpha_0, \beta_0)$ = (0, 13.94, 343.4, 347) for c', and (0, 9.853, 349.7, 320.4) for ϕ' respectively. Note that the site data should be transformed into standard normal space through the isoprobabilistic transform, before applying Equation (3) and Equation (4). The isoprobabilistic transform is done by $y = \Phi^{-1}(F(x))$, where x is the data in the original space, F is the cumulative distribution function of x, and Φ^{-1} is the inverse cumulative distribution function for standard normal. Another remark is that the equations assume that c' and ϕ' are independent (equations for correlated c'- ϕ' are under development).

Sensitivity study of the Bayesian updating formulae indicated that 5 site data points maybe sufficient to bring a systematic deviation of the posterior PDF from the regional PDF, if the site condition does deviate from the regional average. To further improve the efficiency of Bayesian updating (i.e. larger shift of posterior PDF with a smaller amount of site data), the natural starting point is to improve the prior PDF. The prior PDF changes according to the grouping criteria of the 'sites'. For example, instead of grouping the data according to designated zone, grouping by individual slopes can be explored. Another research area is to incorporate the categorical information into the prior PDF. In Phoon et al. (2022), this challenge is referred to as 'mixture of categorical and numerical data of varying proportions in high random

dimensional space'. The data-likelihood may also be improved. A possible way to proceed is to extract data points in the regional database having a high similarity to the site data points, and augment the site data with the extracted data points in the likelihood function.

4 DESIGN CHART METHOD FOR EFFICIENT DESIGN OF ULTIMATE LIMIT STATE

Amongst the multitude of probabilistic approaches, Monte Carlo Simulation (MCS) should be the most well-known and conceptually straightforward, in which the values of soil properties are sampled repeatedly form the corresponding PDF, with the PDF of the structural performance evaluated accordingly. However, MCS is not very efficient when applied into reliability-based design, because MCS typically requires thousands of simulations, and MCS needs to be rerun every time when the design parameters are adjusted.

Meanwhile, first-order reliability method (FORM) is another popular and intuitive probabilistic approach. The focus of FORM is on the reliability index β, which is a 'measure of safety with respect to overpassing the limit state'. In particular, β represents the distance between the mean values of the random variables to the closest point on the limit state surface (LSS), scaled by the standard deviations of these variables. Failure probability P_f is related approximately to β by $P_f \approx \Phi(-\beta)$, where Φ is the cumulative distribution function of standard normal.

Based on the FORM concepts, the authors developed a design chart method for efficient reliability design of ultimate limit state (Lo et al. 2025), which are shown in Figure 6 for Hong Kong CDG and Hong Kong colluvium respectively. First, the regional PDF of c'-ϕ' parameters can be plotted as a series of isodensity locus (blue lines), with each locus having the same scaled distance from the mean values. On each isodensity locus, there are 6 testing points (black squares). Each testing point corresponds to an effective stress level, and the point has the lowest shear strength among the whole locus. In other words, if the Factor of Safety (FOS) of the design is larger than 1.0 for all 6 testing points on the same locus (with a SD of β), then the LSS of the design should lie beyond the locus, and the reliability index of the design is larger than β. If one needs the reliability index of the design to be exactly β, the design parameters can be adjusted until the minimum FOS of the 6 testing points is exactly 1.0. Figure 7 illustrates the design chart concept. One may, with caution, further simplify the reliability design process by selecting lesser number of testing points.

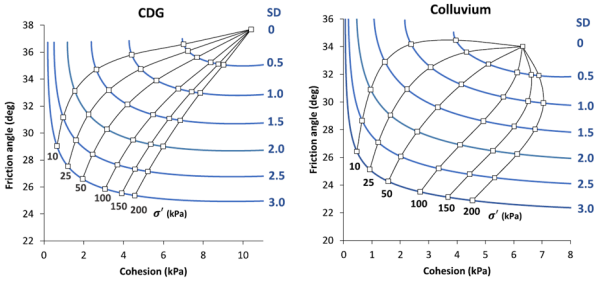

Figure 6. Design charts for Hong Kong CDG and Colluvium.

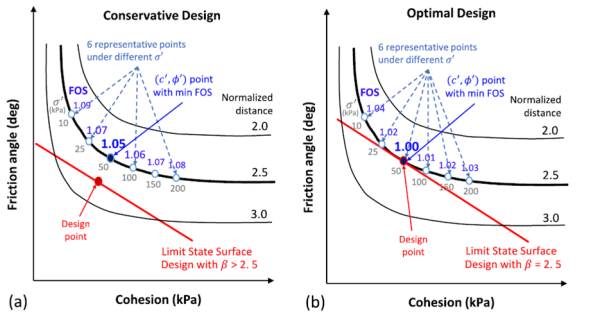

Figure 7. Application of design chart for reliability assessment with target reliability index of 2.5. (left) conservative design; (right) optimal design.

The presented design charts are derived from the regional PDF. It is also possible to use the Bayesian updated PDF for design, by suitable adjustment of the c'-ϕ' points obtained from the design chart. A simple adjustment method is by matching the scaled distances:

$$c_{design} = \frac{\sigma_{c,new}}{\sigma_c}(c_{chart} - \mu_c) + \mu_{c,new} \quad (5)$$

where c_{chart} is the testing point from the design chart; $\mu_{c,new}$ and $\sigma_{c,new}$ are the Bayesian updated mean and SD, evaluated from Equation (2) and Equation (3). Similar formula also applies for ϕ'.

5 RELIABILITY-BASED DESIGN OF SHALLOW FOOTING

This section brings the above reliability approaches together through a shallow footing design example. Assume the shallow footing is square in shape with width B, is located at the surface with loading (q) of 3000kN and no surcharge. The soil beneath the footing is Hong Kong CDG with bulk unit weight 19kNm^{-3} and a thickness of 15m. Groundwater is located at the ground surface. The design load (q_{load}) is q/B^2, and the design bearing capacity is:

$$q_{ult} = 0.5\gamma' B s_\gamma N_\gamma + s_c N_c c' \quad (6)$$

If the target reliability index is 2.5 (i.e. target failure probability of 0.0062), the testing (c', ϕ') point of (2.5kPa, 28.4°) is selected from the design chart in Figure 6, under the stress level of 50kPa. Design width B is then adjusted until the design load equals to design capacity, leading to B_{design} = 3.35m, with design load of 267kPa. Under footing width of 3.35m, Monte Carlo Simulation of size 10000 shows that the failure probability that $q_{ult} < q_{load}$ is 0.0068, which closely matches with the target failure probability.

Next, the serviceability limit state for the same footing scenario is considered, with the following formula used for footing displacement:

$$\delta = \frac{q_{load} B}{E}(1 - \nu^2) I_s \mu_1 \quad (7)$$

where soil Poisson's ratio ν taken as 0.2; I_s = 0.82 for rigid square footing; soil thickness factor μ_1 conservatively taken as 0.7 for square footing. Assume the SLS displacement requirement is 50mm, and the target reliability index is 1.5. The quantile for β of 1.5 is $\Phi(-1.5)$ = 6.7%, and based on the distribution of Young's modulus in Figure 2, the corresponding quantile of E is about 10.1MPa. B is then adjusted until δ equals to 50mm, which leads to B_{design} of 3.28m. Considering both the ULS and SLS requirements, the larger B_{design} out of the two (3.35m) is selected. Apart from using Equation (7) for the SLS design, it is also possible to use adopt numerical methods such as finite difference method, together with soil models

which can account for the non-linearity in soil stiffness. For such case, the PDF of the elasticity parameter A in Figure 2 can be more relevant.

Furthermore, assume five soil samples (n = 5) are taken from the site with multi-stage CU tests performed, and the following (c', ϕ') pairs are obtained: (13KPa, 40°); (20KPa, 33.7°); (5kPa, 46.3°); (8.2kPa, 36.8°) and (18kPa, 43.2°). The mean (c', ϕ') of the site data is (12.8kPa, 40 °), which is slightly higher than the regional mean of (11.9kPa, 37.6°). The transformed data in the standard normal space are (0.18, 0.46); (0.81, -0.75); (-1.34, 1.67); (-0.41, -0.15) and (0.65, 1.08) respectively. Therefore, the sample mean ($\bar{y}$) and sample variance (s_y) of the (transformed) site data are (-0.023,0.462) for c' and (0.769, 0.923) for ϕ' respectively. Applying Equation (3), ($\mu_n, \lambda_n, \alpha_n, \beta_n$) are (0.014, 18.9, 345.9, 348.1) for c' and (0.155, 14.9, 352.2, 322.6) for ϕ' respectively. Finally, applying Equation (2) leads to the Bayesian updated mean and updated SD, which are (12.1kPa, 7.6kPa) for c' and (38.4°, 5.14°) for ϕ' respectively.

Based on the Bayesian updated statistics, the testing (c', ϕ') point in the design chart, which is (2.5kPa, 28.4°), can be adjusted by Equation (5) into a slightly higher value of (2.7kPa, 29.3°). Again, the design width B is adjusted until the design load equals to the design capacity, leading to B_{design} = 3.17m. After Bayesian updating with the site data, the design footing area is reduced by 10.5% while achieving the same target reliability index. In a similar spirit, the distribution of Young's modulus E can also be Bayesian updated, provided that the prior PDF of E is available.

6 RELIABILITY-BASED DESIGN OF SOIL NAILED SLOPES

Soil nailing is a widely used method in Hong Kong to improve the slope stability, where the main cause of slope failures is due to weakening by rainfall infiltration. This section aims to illustrate how to perform efficient reliability-based design for slopes with soil nails. The stabilization forces provided by the soil nails are modelled as point loads on the slope surface. To evaluate the point loads, recommendations of Geoguide 7 (GEO 2017) are followed, with three types of forces being considered. The first force is the allowable pullout resistance provided by soil-grout bond length in passive zone, evaluated as:

$$T_{SG} = \frac{(c' P_c + 2D\sigma_v' \mu^*)L}{F_{SG}} \quad (8)$$

where c' = effective cohesion of soil; P_c = outer perimeter of cement grout sleeve; L = bond length of soil nail in passive zone; D = outer diameter of cement grout sleeve; σ_v' = vertical effective in soil at mid-depth of soil nail in passive zone,; μ^* = coefficient of apparent friction of soil, can be taken as $\tan\phi'$ of soil for a 'drill-and-grout' nail with irregular surface texture; F_{SG} = factor of safety against pullout failure (1.5 for soil nails bonded in weathered granite or volcanic rocks). An important note is that T_{SG} is a random variable, as it depends on the c'- ϕ' of soil. The second force is the allowable pullout resistance provided by grout-reinforcement bond length in passive zone:

$$T_{GR} = \frac{2.25\eta_1\eta_2 f_{ctd} P_r L}{F_{GR}} \quad (9)$$

where η_1 = coefficient related to the quality of the bond condition; η_2 = coefficient related to the steel bar diameter; f_{ctd} = design value of concrete tensile strength; Pr = effective perimeter of soil-nail; L = bond length of soil-nail in the passive zone; F_{GR} = factor of safety against pullout failure (2.0). The third force is the allowable tensile capacity of soil-nail:

$$T_T = \frac{f_y A}{F_T} \quad (10)$$

where f_y = Characteristic yield strength of soil-nail; A = effective cross-sectional area of soil-nail; F_T = Factor of safety against tensile failure of soil-nail. All three types of soil nail forces are normalized by the horizontal spacing of soil nails, and the stabilization force provided by a row of soil nail is taken as the minimum of the three normalized forces. An Excel Spreadsheet tool is developed by the authors to evaluate the stabilization force following the above formulae.

The SLOPE/W software is adopted for limit equilibrium analysis of slope stability. The slope model is shown in Figure 8. The slope is around 70 meters long and 18 meters high at its highest point, and slope degree is around 50°. The soil is primarily Hong Kong CDG. The slope has a highest Consequence-to-life Category in accordance to the Geoguide 7. The groundwater level is set to about 1/3 of the slope height, as evaluated by the wetting band method under the 1-in-10 year rainstorm condition. Slip surfaces are specified with entry-exit method, and the Morgenstern–Price method is adopted with half-sine interslice force function. Monte Carlo Simulation with size 5000 shows that the mean FOS is 1.415, SD of FOS is 0.325, and failure probability is 0.08 (i.e. reliability index of 1.41), suggesting the need of slope improvement by soil nails.

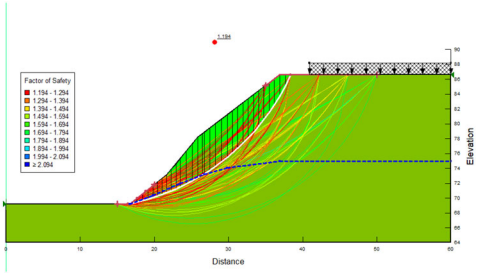

Figure 8. Slope model prior to installing soil nails

Assuming a target reliability index of 2.5 (i.e. target failure probability of 0.0062), the 6 testing (c', ϕ') points are selected accordingly from the design chart. For each suggested configuration of soil nails, the slope FOS are evaluated 6 times under the testing (c', ϕ') points, The aim is to find a soil nail configuration, such that the minimum slope FOS is 1.0 (or slightly exceeds 1.0) under the 6 testing points. Following this methodology, the proposed soil nail plan is shown in Figure 9. The bottom four rows of soil nails are 13 m long, while the top two rows are 9 m long. The soil nail horizontal spacing is 2.5m. The minimum slope FOS is 1.02 for the 6 testing (c', ϕ') points, therefore it satisfies the criteria of the design chart method. For validation, Monte Carlo Simulation of the soil-nailed slope shows that the mean FOS is 1.81, SD of FOS is 0.38 and failure probability is 0.0078, which is indeed close to the target failure probability.

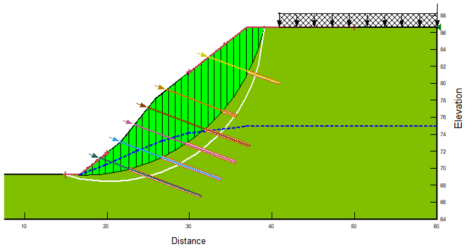

Figure 9. Proposed soil nail design with groundwater 1/3 of slope height.

Since assigning groundwater level being 1/3 of the slope height can be conservative (i.e. not all the rainfall infiltration

can reach the main groundwater table), and cannot account for the development of transient groundwater, a seepage analysis is carried out by SEEP/W software, using the rainfall intensity of 125mm/hr, rainfall duration of 6 hours, soil saturated permeability of $3.5x10^{-5}$m/s, and the soil-water characteristic curve provided in GEO Report No. 193. Following the same reliability-based design process, the proposed soil nail configuration is shown in Figure 10, together with the porewater pressure. The bottom four rows of soil nails are 9 m long, while the top two rows are 8 m long. The soil nail horizontal spacing remains 2.5m. For the same target reliability index of 2.5, the minimum slope FOS is 1.021 for the 6 testing (c', ϕ') points, therefore the design chart criteria is satisfied. Monte Carlo Simulation under this soil nail configuration shows that the mean FOS is 1.82, the SD of FOS is 0.385 and failure probability is 0.0078. The FOS distribution for this soil-nailed slope is shown in Figure 11. Therefore, by performing a more detailed groundwater modelling, it is possible to further reduce the length of soil nails in the design. In this case, the length of soil nails is reduced by 25% while achieving the same target reliability index. Conceptually, it is possible to perform Bayesian updating to refine the c'- ϕ' distribution and thus the soil nail design, and this is a scope of further research.

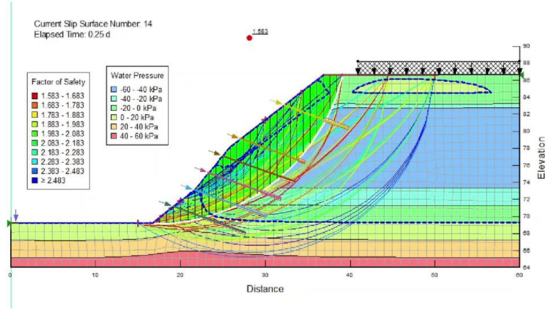

Figure 10. Proposed soil nail design with groundwater from seepage analysis.

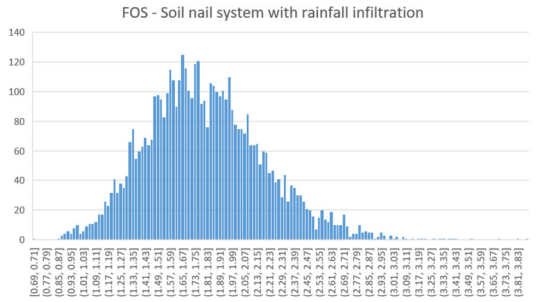

Figure 11. Slope FOS distribution under the proposed soil nail design.

7 CONCLUSIONS

This paper discussed some challenges related to the reliability-based design in geotechnical engineering, and how to utilize the geotechnical soil test database to address those challenges. In particular this paper focus on the multi-stage CU test database maintained by Hong Kong GEO, with over 3000 sets of test data. Regional PDF for shear strength parameters c' and ϕ' are established for various Hong Kong soil types. Moreover, by digitizing the entire stress path of the multi-stage CU test, and by calibrating the soil constitutive parameters, the PDF for soil stiffness parameters (Young's modulus, small-strain shear modulus) and critical state parameters can also be formulated.

Soil test data obtained at the site can be augmented with the regional PDF through the Bayesian updating, leading to a refined PDF of soil properties. The prior PDF is formulated based on a Hierarchical Bayesian model. Furthermore, simplified expressions are derived to implement the Bayesian updating conveniently, which considers the sample mean, sample variance and number of the site data.

Next, a shallow footing example is presented to illustrate the reliability-based design of ultimate limit state (bearing capacity failure) and serviceability limit state (excessive settlement). A design chart method is utilized to accelerate the reliability-based design process, bypassing the need to carry out the computationally intensive Monte Carlo Simulation. Furthermore, the footing design can be revised based on the newly available site data, which may lead to a less costly design. Another application example is the reliability-based design of slopes with soil nails, where the stabilization force is mainly controlled by the pullout resistance at the soil-grout interface, which is treated as a random variable. The analysis also utilizes the design chart method, to propose a soil nail configuration which meets the target reliability index of 2.5.

Overall, this study constitutes a solid step towards building a data-centric platform for geotechnical data, which can further promote the data-driven geotechnical design. Although this study focuses on the multi-stage CU test data, research is ongoing to further compile the other field test and laboratory test data of Hong Kong soils. For example, soil permeability can be evaluated from the isotropic consolidation stage in the triaxial test data. Many sets of triaxial test data are accompanied by the particle size distribution sieve test. There are also recent test data on the dynamic properties of Hong Kong soil, including shear wave velocity and modulus degradation curve. The goal is to integrate the geotechnical data of various scales into a central data platform.

8 REFERENCES

Chan, C., Wong, L., Leung, W., Chung, P., Lo, M. K., and Leung, Y. 2022. Development of regional soil shear strength database and its application in probabilistic analysis of slope stability. *Proc. 8th International Symposium on Geotechnical Safety and Risk (ISGSR)*, Newcastle, Australia.

GEO 2017. *Geoguide 7*: *Guide to soil nail design and construction*. Hong Kong Geotechnical Engineering Office.

GEO 2020. *Geoguide 1: Guide to retaining wall design.* Hong Kong Geotechnical Engineering Office.

Jefferies, M. G. 1993. Nor-Sand: a simple critical state model for sand. *Géotechnique* 43(1), 91-103.

Lo, M. K., and Leung, Y. F. 2025. Simplified expressions for hybridiszing regional and site-specific soil shear strength information for cost-effective reliaiblity-based design. *Proc. 9th International Symposium for Geotechnical Safety and Risk (ISGSR)*, Oslo, Norway.

Lo, M. K., Leung, Y. F., Chan, C. L., and Sze, E. H. Y. 2024. Reappraisal of reliability of a slope through hybridisation of regional and site-specific soil shear strength information. *Canadian Geotechnical Journal* 62, 1-24.

Lo, M. K., Leung, Y. F., and Wang, M. X. 2025. Data-enhanced design charts for efficient reliability-based design of geotechnical systems. *Structural Safety* 112, 102527.

Phoon, K. K., Ching, J., and Shuku, T. 2022. Challenges in data-driven site characterization. *Georisk: Assessment and Management of Risk for Engineered Systems and Geohazards* 16(1), 114-126.

Wang, Y., Akeju, O. V., and Cao, Z. 2016. Bayesian Equivalent Sample Toolkit (BEST): an Excel VBA program for probabilistic characterisation of geotechnical properties from limited observation data. *Georisk: Assessment and Management of Risk for Engineered Systems and Geohazards* 10(4), 251-268.